The University of Tehran Press

Pollution

Print ISSN: 2383-451X
Online ISSN: 2383-4501

https://jpoll.ut.ac.ir/

Comparative Kinetic Evaluation of Resin Immobilized TiO_2 and ZnO Photocatalysts in a Continuous Fixed-Bed System for Industrial and Food Wastewater Treatment

Euis Nurul Hidayah[1]✉ | Nur Laili Alfiatin Mukharomah[2] | Ika Nawang Puspitawati[3] | Moch. Andy Wibisono[2] | Arya Darmawan[2]

1. Department of Environmental Engineering, Universitas Pembangunan Nasional Veteran Jawa Timur, Surabaya, 60294, Indonesia
2. Environmental Recearch Center, Universitas Pembangunan Nasional Veteran Jawa Timur, Surabaya, 60294, Indonesia
3. Department of Chemical Engineering, Universitas Pembangunan Nasional Veteran Jawa Timur, Surabaya, 60294, Indonesia

Article Info

Article type:
Research Article

Article history:
Received: 2 Jan 2026
Revised: 29 May 2026
Accepted: 3 Sep 2026

Keywords:
COD,
Hexavalent Chromium,
Photocatalysis,
Semiconductor Catalyst,
Wastewater

ABSTRACT

Electroplating wastewater contains toxic Cr^{6+}, while tofu wastewater has a high organic load that degrades water quality. Advanced oxidation processes (AOPs) based on photocatalysis have been extensively developed, including fixed-bed reactors. However, the application of continuous systems remains limited due to the prevalence of batch scale studies, uneven flow distribution, and limited contact between pollutants and the photocatalyst. This study employs a continuous fixed-bed photocatalytic reactor as the primary innovation to address these limitations. The performance of resin immobilized TiO_2 and ZnO was evaluated for Cr^{6+} removal and COD reduction. The resin immobilized TiO_2 and ZnO was synthesized via a stirring method under dark conditions. Mass variations of 10, 20, and 30 g were used in the reactor which was operated under UV-C irradiation (40 W/m²) at a flow rate of 60 mL/min. Samples were analyzed from 0 to 180 minutes for Cr^{6+}, COD, and pH parameters. The results showed that resin immobilized ZnO provided better performance, with Cr^{6+} removal of 71.36% and COD reduction of 92.61%, compared to resin immobilized TiO_2, which achieved 70.80% and 84.89%. Acidic conditions enhanced process effectiveness through the formation of hydroxyl radicals and redox reactions. Kinetic analysis indicated that the COD reduction followed first-order kinetics, whereas Cr^{6+} removal followed second-order kinetics, reflecting differences in reaction mechanisms. Overall, the developed continuous fixed-bed system demonstrated stable performance and holds potential for sustainable wastewater treatment applications.

Cite this article: Hidayah, E. N., Mukharomah, N. L. A., Puspitawati, I. N., Wibisono, M. A., & Darmawan, A. (2026). Comparative Kinetic Evaluation of Resin Immobilized TiO_2 and ZnO Photocatalysts in a Continuous Fixed-Bed System for Industrial and Food Wastewater Treatment. *Pollution*, 12(3), 846-864.
https://doi.org/10.22059/poll.2026.409175.3258

 Publisher: The University of Tehran Press.
DOI: https://doi.org/10.22059/poll.2026.409175.3258

INTRODUCTION

Population growth and rapid industrialization have increased the concentration of organic pollutants, heavy metals, inorganic compounds, and various other complex compounds in surface water, groundwater, and wastewater (Ren et al., 2021). Water body pollution by organic compounds has even become a global environmental issue (Miri-Jahromi et al., 2022) (Lee et al., 2022). In Indonesia, industrial developments such as metal plating and tofu processing contribute to this problem. Metal plating waste contains Cr^{6+}, which is toxic, carcinogenic, and difficult to degrade naturally (Elystia et al., 2021) and has the potential to contaminate water

*Corresponding Author Email: *euisnh.tl@upnjatim.ac.id*

bodies and disrupt ecosystem balance (Wise et al., 2022b). On the other hand, tofu wastewater has a very high organic load, with a BOD of 4,194.7 mg/L and a COD of 10,564.7 mg/L, which can reduce the carrying capacity of aquatic environments if not properly treated (Azzahra & Rahman, 2025).

Various wastewater treatment technologies, such as biological processes, oxidation, activated carbon adsorption, and membrane filtration, have been widely applied. These methods are known for their high surface area, large number of active pores, relatively low operational costs, and ability to minimize byproduct formation (Zakria et al., 2021). However, when used individually, their effectiveness remains limited in addressing complex pollutants, particularly heavy metals (Iyyappan et al., 2024). This situation has driven the development of more effective alternative technologies, one of which is photocatalysis. Photocatalysis enables the oxidative degradation of various pollutants through the formation of reactive free radicals resulting from the excitation of semiconductors by light (Cloteaux et al., 2014).

Semiconductor materials such as TiO_2 and ZnO have been extensively studied due to their high catalytic activity, good stability, and lack of secondary pollution (Qu et al., 2025) (Zheng, 2022) (Ge et al., 2022) (Rangarajan et al., 2022). However, the use of photocatalysts in slurry form poses challenges during the post-process catalyst separation stage, leading to increased operational costs and potential loss of catalyst material. Therefore, photocatalyst immobilization is a more practical approach. This method not only eliminates the need for filtration but also reduces exposure to nanoparticles (Cloteaux et al., 2014). Ion-exchange resins serve as a relevant support material in this system. Resins are cross-linked polymers with active groups capable of ion exchange, and they possess good physical and chemical stability (León-condés et al., 2022). In addition to serving as a photocatalyst support, the resin also provides adsorption sites that enable initial interactions between pollutants and the material. This combination creates a synergistic mechanism between adsorption and photodegradation, where pollutants are first bound to the resin and then degraded on the catalyst surface. This approach not only enhances process efficiency but also helps maintain catalyst stability and reduce the loss of active material (Kotze et al., 2016) (Zeng et al., 2023). The effectiveness of this synergy has been demonstrated in several studies, where ZnO-immobilized resin showed better performance than TiO_2 in pollutant removal (Hidayah et al., 2022).

The need to reduce concentrations of heavy metals and organic pollutants more effectively has driven the development of photocatalytic methods that offer advantages over conventional methods such as chemical precipitation, adsorption, and ion exchange. Photocatalysis works by utilizing UV light energy to activate semiconductor catalysts such as TiO_2 and ZnO, thereby generating reactive radicals, particularly hydroxyl radicals (•OH), which are capable of reducing Cr^{6+} to the less toxic Cr^{3+} (Illahi et al., 2020). When absorbing light energy corresponding to its bandgap, the semiconductor generates charge pairs that trigger oxidation-reduction reactions, while the resin acts as a catalyst support that enhances stability and active surface area, thereby accelerating the photocatalytic process (Ramadhika et al., 2021, Chakravorty & Roy, 2024). The effectiveness of this technology's integration is reinforced by the research of Zahrah et al. (2025), which demonstrates that ZnO immobilized on resin can remove up to 96% of Cr^{6+} from nickel industrial wastewater under sunlight exposure (Zahrah et al., 2025).

Nevertheless, fixed-bed photocatalytic systems still face challenges, particularly regarding mass transfer barriers and uneven light distribution (Yang & Chen, 2024). However, from a process engineering perspective, this configuration still offers advantages such as ease of operation and the absence of the need for catalyst separation. TiO_2- and UV-based fixed-bed reactors have been extensively studied, including in hydraulic analyses via residence time distribution (RTD) and modeling that accounts for mass transfer and reaction kinetics (Ananpattarachai & Kajitvichyanukul, 2014) (Cloteaux et al., 2014).

Most previous studies were still conducted in batch systems, which have limitations in

operational continuity and treatment capacity. Therefore, the use of continuous fixed-bed systems becomes more relevant for real-world applications. This system enables sustainable wastewater treatment in larger volumes, maintains operational stability, and enhances contact efficiency between pollutants and the catalyst. Additionally, catalyst immobilization in continuous systems reduces the need for separation and regeneration, thereby potentially lowering operational costs. Based on this, this study aims to evaluate and compare the performance of resin immobilized TiO_2 and ZnO photocatalysts in the removal of Cr^{6+} and reduction of COD. Electroplating wastewater and tofu wastewater were selected as representative heavy metal and organic pollutants. This study employs a continuous fixed-bed photocatalytic reactor as the primary approach to enhance the efficiency and sustainability of the wastewater treatment process.

MATERIAL & METHODS

This study investigated electroplating wastewater from Gresik and tofu wastewater from Surabaya, Indonesia, with all experiments conducted at the Environmental Engineering Laboratory, Universitas Pembangunan Nasional "Veteran" Jawa Timur, Indonesia.

Materials and Preparation of Resin-Immobilized Photocatalysts

The research began with the preparation of resin immobilized using TiO_2 and ZnO semiconductor catalysts, resulting in resin immobilized TiO_2 and resin immobilized ZnO materials. These materials were subsequently applied in the wastewater treatment process through photocatalysis. The preparation process of resin immobilized TiO_2 and ZnO is presented in Figure 1.

An immobilization process was performed by dispersing 30 g of Dowex anion exchange resin in 1000 mL of deionized (DI) water, followed by the addition of 30 g of TiO_2 (molecular weight: 79.90 g·mol^{-1}) and 30 g of ZnO (molecular weight: 81.39 g·mol^{-1}) in a 2000 mL beaker (Pyrex). The suspension was batch-stirred for 72 h under dark conditions to prevent premature photocatalytic activation and to promote the adsorption of semiconductor particles onto the resin surface. After stirring, the mixture was filtered to separate the resin immobilized photocatalyst

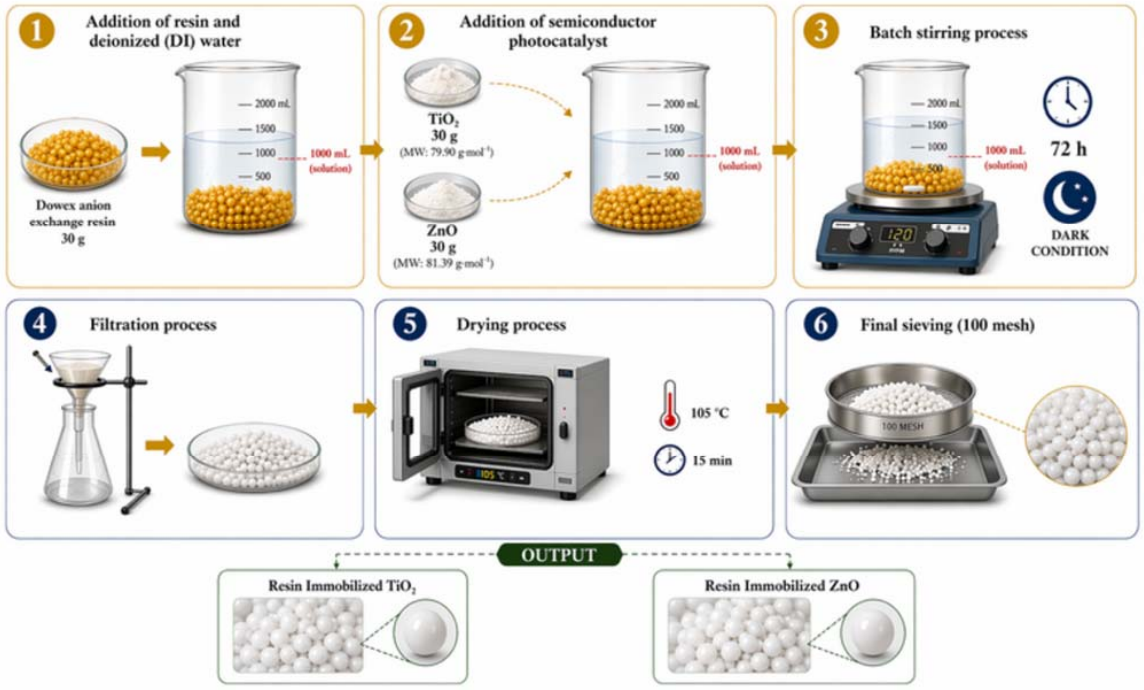

Fig. 1. The process of preparing resin immobilized photocatalyst TiO_2 and ZnO materials

from the supernatant containing unbound semiconductor particles. The recovered material was then dried in an oven at 105°C for 15 min to remove residual moisture. Subsequently, a final sieving step using a 100-mesh screen was applied to remove loosely attached semiconductor particles, ensuring that only firmly immobilized TiO_2 and ZnO remained on the resin surface.

Photocatalytic Reactor Setup and Experimental Procedure

The reactor was constructed from 0.018 m thick plywood with the inner surfaces lined with aluminum foil to enhance the reflection of UV-C light at an intensity of 40 W/m² irradiation toward the glass tubes. Photocatalytic experiments were conducted using a continuous fixed-bed reactor consisting of three vertical glass tube columns, each with a height of 0.5 m, an inner diameter of 0.008 m and an outer diameter of 0.010 m, enclosed within a reactor box of 0.7 m in length. A UV-C light at an intensity of 40 W/m² was positioned at a distance of 10 cm from the glass tubes, and the columns were packed with resin immobilized photocatalysts (TiO_2 or ZnO) at varying masses of 10, 20, and 30 g to evaluate the effect of immobilized resin mass on degradation performance. Prior to operation, the fixed-bed columns were rinsed with deionized water to remove loosely attached particles and maintain bed stability. Electroplating wastewater and tofu wastewater were treated separately and continuously fed into the reactor at a flow rate of 60 mL/min using a calibrated submersible pump (EU Plug 220 V IPX8 40W DHP, China) to ensure stable flow conditions and optimal mass transfer. Each column was equipped with a UV-C light at an intensity of 40 W/m² (λ 100–280 nm) positioned parallel to the column to provide uniform irradiation and ensure effective activation of the photocatalyst throughout the bed. During operation, the reactor was covered to minimize interference from external light sources. The hydraulic retention time (HRT) was controlled based on reactor volume and influent flow rate to ensure sufficient contact between pollutants and the catalyst surface. All experiments were conducted without the addition of external chemicals, allowing a clearer comparison of TiO_2 and ZnO performance in Cr^{6+} removal and COD reduction, as well as the influence of resin immobilized photocatalyst mass and irradiation time on overall reactor performance.

Analytical Methods

Samples were collected at predetermined reaction intervals (0, 5, 15, 30, 45, 60, 75, 120, and 180 min) to systematically evaluate the photocatalytic degradation process. The concentration of hexavalent chromium (Cr^{6+}) in electroplating wastewater was determined using a double-beam UV–Vis spectrophotometer (DUVL7, China) in accordance with SNI 6989.71:2009. Chemical oxygen demand (COD) in tofu wastewater was measured using the closed reflux colorimetric method based on SNI 6989.02:2019. The pH was monitored using a calibrated pH meter (Eutech, Thermo Scientific, Germany) following SNI 6989.11:2019 to assess its role in influencing photocatalytic activity. All analytical procedures adhered to standardized methods to ensure data validity and comparability. Experiments were conducted in triplicate, and the results are presented as mean values to enhance data reliability and minimize experimental uncertainty.

Kinetic Analysis of Photocatalytic Reactions

The kinetics of photocatalytic degradation were evaluated by analyzing the variation in pollutant concentration as a function of reaction time. The kinetic behavior was analyzed using the Langmuir–Hinshelwood (L–H) model, which is widely applied to describe heterogeneous photocatalytic reactions (Hikmah et al., 2025). This model represents the relationship between reaction rate, pollutant concentration, and surface adsorption on the photocatalyst.

$$r = -\frac{dC}{dt} = \frac{kKC}{1 + KC}$$

where r is the reaction rate (mg/L/min), C is the pollutant concentration (mg/L), k is the intrinsic reaction rate constant, and K is the Langmuir adsorption constant.

At relatively low pollutant concentrations $(KC \mid 1)$, the L–H equation can be simplified into a pseudo-first-order kinetic model:

$$-\frac{dC}{dt} = k_1 C$$

After integration, the equation becomes:

$\ln\left(\frac{C_0}{C}\right) = k_1 t$ where C_0 is the initial pollutant concentration and k_1 is the pseudo-first-order rate constant (1/min).

For systems exhibiting more complex surface interactions, the reaction kinetics may follow a pseudo-second-order model:

$-\frac{dC}{dt} = k_2 C^2$ The integrated form of this equation is given by:

$$\frac{1}{C} = k_2 t + \frac{1}{C_0}$$

where k_2 is the pseudo-second-order rate constant (L/mg/min).

The reaction order was determined based on the linearity of the plots of $\ln(C_0 / C)$ versus time for the pseudo-first-order model and $1/C$ versus time for the pseudo-second-order model. The rate constants were obtained from the slopes of the corresponding linear regressions, while the coefficient of determination (R^2) was used to evaluate the goodness of fit of each kinetic model.

RESULTS AND DISCUSSIONS

Characteristic of Wastewater

Tofu processing wastewater is classified as industrial wastewater rich in organic matter generated from tofu production activities and characterized by high concentrations of biodegradable organic compounds (Hardyanti et al., 2023). This wastewater has a COD concentration of 1677.67 mg/L and an acidic pH of 4.10, indicating a high organic load. The elevated COD level is primarily attributed to dissolved proteins, carbohydrates, and lipids released during the soybean soaking, boiling, and coagulation processes (Hardyanti et al., 2023) (Prawati et al., 2019). If discharged without proper treatment, the high organic content can lead to oxygen depletion in receiving water bodies, induce anaerobic conditions, and cause severe environmental pollution (Hardyanti et al., 2024). These characteristics suggest that tofu wastewater is highly suitable for treatment using photocatalytic oxidation processes, which are effective in degrading organic pollutants.

In contrast, electroplating wastewater is a byproduct of the metal coating process and is known to contain high concentrations of heavy metals, particularly hexavalent chromium (Cr^{6+}) (Z. Li & Du, 2025). Based on analytical results, the initial Cr^{6+} concentration was 1009.40 mg/L, with a pH of 3.20. Under acidic conditions, chromium is predominantly present as dichromate ions ($Cr_2O_7^{2-}$) rather than chromate ions (CrO_4^{2-}) (Szabó et al., 2018). These chromium species are highly toxic and carcinogenic, posing serious risks to human health, particularly through inhalation exposure, and increasing cancer risk due to environmental contamination (Prasad et al., 2021) (Jiang et al., 2019). The acidic conditions and the presence of soluble Cr^{6+} species favor photocatalytic reduction processes, making this wastewater suitable for treatment using semiconductor-based photocatalysts.

The performance of the photocatalytic treatment for both tofu and electroplating wastewater, including changes in pH and pollutant removal efficiency, is summarized in Table 1.

Photocatalytic Mechanisms and pH Effects in Resin Immobilized TiO_2 and ZnO for Wastewater Treatment

One of the key factors influencing photocatalyst performance is pH. Based on Figure 2, the pH values after treatment remained within the acidic range, with electroplating wastewater exhibiting pH values of 3.2–4.4 for resin immobilized photocatalyst TiO_2 and 3.2–6.3 for resin immobilized photocatalyst ZnO. Meanwhile, in tofu wastewater, the pH range for resin immobilized photocatalyst TiO_2 was 3.38–4.10, while that for resin immobilized photocatalyst

Table 1. Performance of Photocatalytic Treatment on Tofu and Electroplating Wastewater

Wastewater Type	Treatment	Parameter	Unit	Initial Value	Final Value	Removal Efficiency (%)
Tofu Wastewater	Resin Immobilized ZnO (30 g ; 180 min)	pH	-	4.10	4.00	-
		COD	mg/L	1677.67	123.95	92.61
	Resin Immobilized TiO_2 (30 g ; 180 min)	pH	-	4.10	3.68	-
		COD	mg/L	1677.67	253.42	84.89
Electroplating Wastewater	Resin Immobilized ZnO (30 g ; 180 min)	pH	-	3.20	5.30	-
		Cr^{6+}	mg/L	1009.4	289,1	71.36
	Resin Immobilized TiO_2 (30 g ; 180 min)	pH	-	3.20	3.30	-
		Cr^{6+}	mg/L	1009.4	294.7	70.80

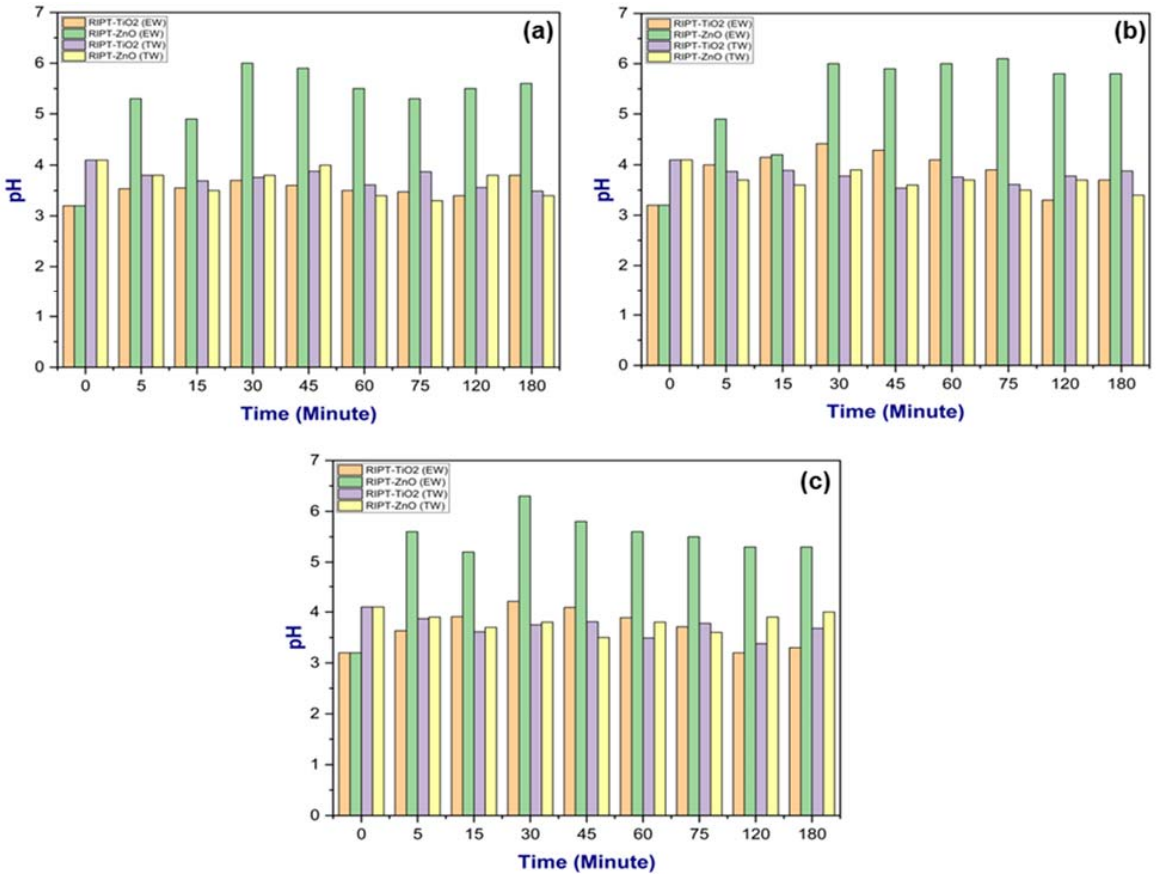

Fig. 2. pH fluctuations during the photocatalytic process in wastewater at different immobilized resin masses: (a) 10 g (b) 20 g and (c) 30 g

ZnO ranged from 3.30 to 4.10. Castiblanco et al. (2021) reported that acidic pH conditions (approximately 3.3) are associated with higher efficiency in hexavalent chromium reduction (Castiblanco et al., 2021). In contrast, Silmina et al. (2023) found that a pH of 5.42 resulted in more effective hexavalent chromium reduction than a pH of 3 (Silmina et al., 2023). These differing findings indicate that photocatalyst effectiveness is strongly influenced by wastewater characteristics and its initial pH conditions.

The final pH of the wastewater after undergoing the photocatalytic process follows the same trend as shown in Figure 2, remaining within the acidic range. This acidification occurs as a result of the photocatalytic reactions, as described by the following equations (Navidpour et al., 2023):

$$Semiconductor + h\vartheta \rightarrow Semiconductor\left(h^{+}_{VB} + e^{-}_{CB}\right) \quad (1)$$

$$h^{+}_{VB} + e^{-}_{CB} \rightarrow heat\left(energy\right) \quad (2)$$

$$H_2O + h^{+}_{VB} \rightarrow \cdot OH + H^{+} \quad (3)$$

These reactions indicate that holes (h^+) generated from electron excitation in the TiO_2 catalyst react with water molecules (H_2O) to produce hydroxyl radicals (•OH) and hydrogen ions (H^+), leading to a decrease in pH and resulting in acidic conditions. However, when resin immobilized ZnO is applied, the final pH of the wastewater tends to remain more stable. This behavior can be explained by the following reaction:

$$ZnO + 2H^{+} \rightarrow Zn^{2+} + H_2O \quad (4)$$

This reaction demonstrates that ZnO can consume the generated H^+ ions, creating a buffering

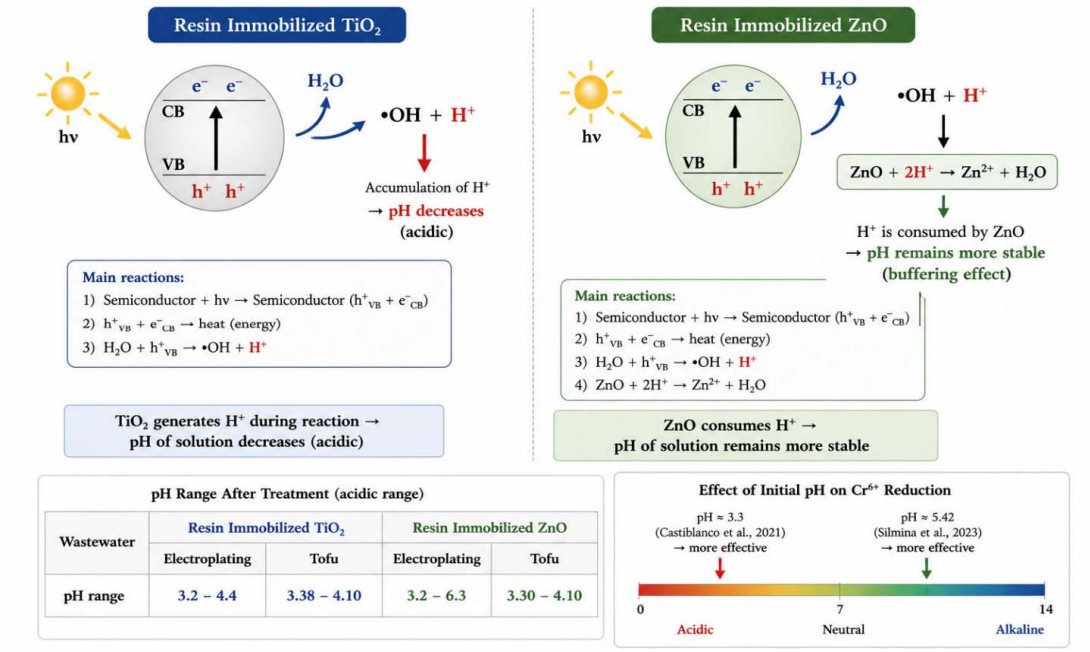

Fig. 3. pH Mechanism in Photocatalysis with Resin Immobilized TiO_2 and Resin Immobilized ZnO

effect that helps stabilize the pH during the photocatalytic process.

Furthermore, resin immobilized proved effective in removing Cr^{6+} from electroplating wastewater and removing COD in tofu wastewater, as illustrated in Figure 4. In electroplating wastewater, Cr^{6+} removal efficiencies ranged from 8.48% to 70.80% for resin immobilized TiO_2 and from 8.52% to 71.36% for resin immobilized ZnO. Meanwhile, in tofu wastewater, COD removal efficiencies ranged from 4.54% to 84.89% for resin immobilized photocatalyst TiO_2 and from 7.19% to 92.61% for resin immobilized photocatalyst ZnO. These results indicate that the immobilized photocatalysts are capable of achieving substantial organic matter removal alongside effective heavy-metal reduction under optimized operating conditions.

Based on Figure 4, the Cr^{6+} removal in electroplating wastewater shows an increasing trend with increasing time across all treatments. The resin immobilized photocatalyst ZnO achieved a removal efficiency of 71.36% at 180 minutes, while the highest removal efficiency, 70.80%, was obtained using resin immobilized photocatalyst TiO_2. These results indicate that the photocatalytic process in electroplating wastewater requires longer times to allow the generated reactive species, such as •OH and $•O_2^-$ radicals, to act effectively in reducing Cr^{6+}. Extending the time enhances process efficiency by providing sufficient duration for photoreduction reactions to occur, enabling more optimal interactions between free electrons and pollutant species (Hidayah et al., 2022). Based on the experimental results, the resin immobilized photocatalyst ZnO at a mass of 30 g with a time of 180 minutes represents the most effective operational condition for Cr^{6+} removal from electroplating wastewater.

The use of resin immobilized photocatalyst ZnO in the photocatalytic process shows higher

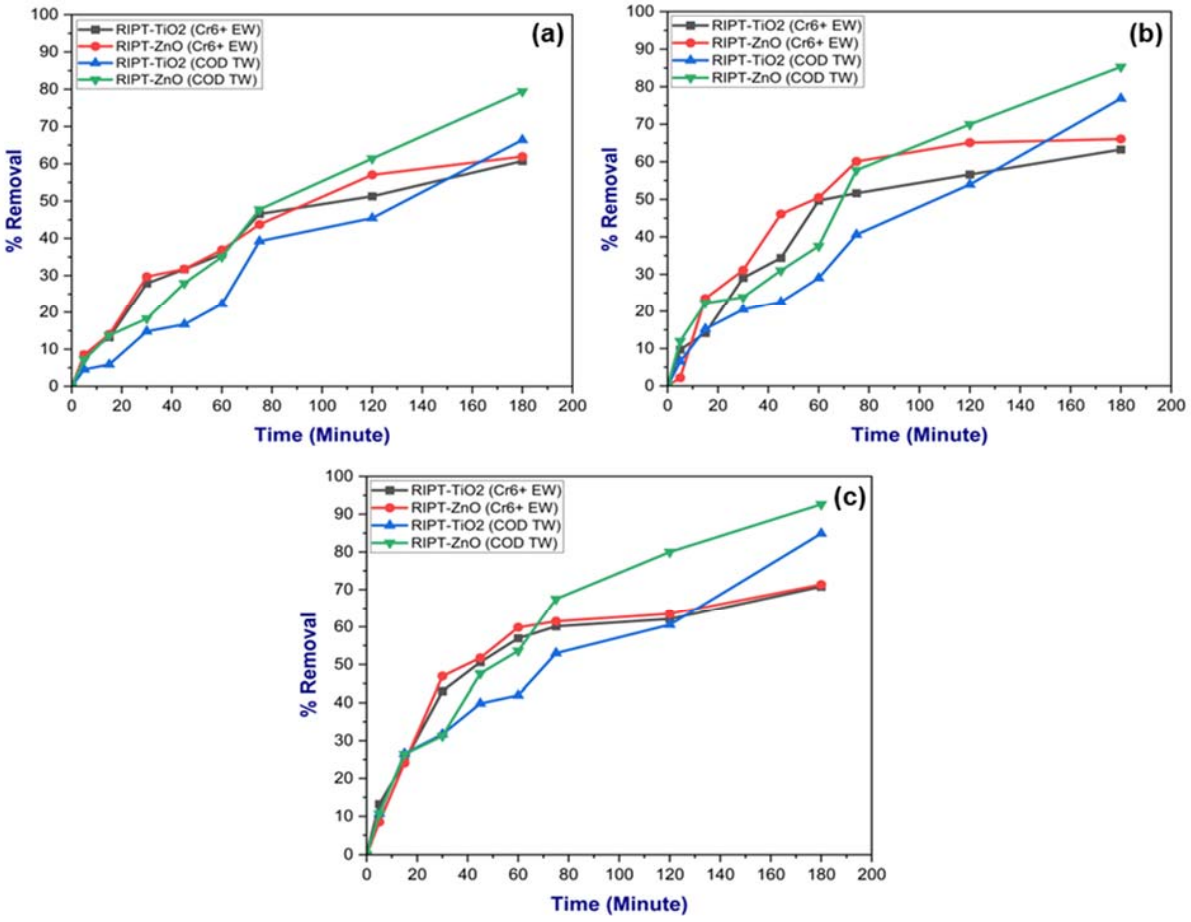

Fig. 4. Percentage removal during the wastewater treatment process using different immobilized resin masses (a) 10 g (b) 20 g and (c) 30 g

effectiveness than resin immobilized photocatalyst TiO_2 in reducing Cr^{6+} concentration in electroplating wastewater. This higher performance can be attributed to the greater adsorption and photocatalytic capacity of resin immobilized photocatalyst ZnO, which enhances the generation of hydroxyl radicals (•OH) and promotes more efficient Cr^{6+} reduction. This difference is closely related to the pH condition of the wastewater. Electroplating wastewater has a pH values of 3.2–4.4 for resin immobilized photocatalyst TiO_2 and 3.2–6.3 for resin immobilized photocatalyst ZnO, which is relatively acidic. These conditions affect the point of zero charge (pHpzc) of each photocatalyst. ZnO generally has a pHpzc in the range of 9.0–9.5, so that at pH values below this, the surface of ZnO becomes positively charged (Fatehah et al., 2014). Since Cr^{6+} ions (e.g., CrO_4^{2-} and $Cr_2O_7^{2-}$) are negatively charged, the electrostatic interaction is enhanced, allowing more effective reduction of Cr^{6+} under acidic to neutral conditions. Conversely, anatase TiO_2 has a pHpzc of around 6.25, so that at pH values above this, its surface becomes negatively charged. Under alkaline or near-alkaline conditions, interactions with negatively charged Cr^{6+} ions are hindered due to electrostatic repulsion, thereby reducing the effectiveness of Cr^{6+} reduction by resin immobilized photocatalyst TiO_2 (Wise et al., 2022a). In addition, the adsorption capacity of resin immobilized TiO_2 is slightly lower than that of resin immobilized ZnO, which also contributes to its comparatively lower performance in acidic electroplating wastewater.

In the tofu wastewater, a similar pattern to that observed in electroplating wastewater was also evident, where the removal efficiencies increased with increasing time across all treatments. The resin immobilized photocatalyst ZnO achieved a removal efficiency of 92.61% at 180 minutes, while the highest removal efficiency for resin immobilized photocatalyst TiO_2 was 84.89% under the same conditions. The reduction of COD in this process is based on the principles of Advanced Oxidation Processes (AOPs) through a photocatalytic mechanism that exploits the generation of highly reactive *hydroxyl radicals* (•OH) (Hikmah et al., 2025). AOPs are capable of producing large quantities of •OH radicals, which serve as very strong oxidants that can non-selectively break down organic pollutants in wastewater (Ul et al., 2023). In heterogeneous photocatalytic AOPs, when a semiconductor catalyst such as TiO_2 or ZnO is irradiated with light of sufficient energy (e.g., UV), photogenerated electron–hole pairs are produced. The photogenerated holes (h^+) oxidize adsorbed water molecules or hydroxide ions to form •OH radicals, while the electrons reduce dissolved oxygen, further contributing to reactive oxygen species formation. These •OH radicals then oxidize organic pollutants into smaller intermediate molecules, and ultimately lead to mineralization producing CO_2 and H_2O (Shan et al., 2023).

ZnO superior performance compared to TiO_2 stems from the differences in their physicochemical properties, such as band gap, charge mobility, and crystal structure. Table 2 summarizes the key parameters of both materials and their relationship to photocatalytic performance.

Although ZnO exhibits good photocatalytic activity under UV light, this material has the drawback of being prone to photocorrosion. This process occurs because the holes (h^+) formed not only react with pollutants but also attack the ZnO structure, leading to the release of Zn^{2+} into the solution ($ZnO + 2h^+ \rightarrow Zn^{2+} + ½O_2$) (Dworschak et al., 2020). Additionally, suboptimal electron–hole pair separation can accelerate recombination and exacerbate the degradation process (X. Li et al., 2023). ZnO photocorrosion is influenced by both pollutant-free conditions (internal mechanism) and the presence of pollutants (external mechanism) (Dimitropoulos et al., 2024). Prolonged UV irradiation (up to 8 hours) can aid in the recovery of the ZnO structure. To mitigate this effect, several solutions have been implemented, such as surface passivation (Taylor et al., 2019), heterojunction formation (Yu et al., 2015), and the addition of noble metals (Ma et al., 2017).

In contrast Di sisi lain, TiO_2 is more stable but has limitations in light absorption due to its relatively large bandgap (~3.2 eV), making it generally active only under UV light. Efforts such as doping, for example with calcium, can alter its electronic structure and narrow the band gap,

Table 2. Comparative analysis of ZnO and TiO_2 properties affecting photocatalytic efficiency

Aspek	ZnO	TiO_2
Element	-	O K Ti K
Weight%	-	58.16 41.84
Atomic%	-	80.63 19.37
Band Gap Energy (eV)	Direct, 3.37 eV	Indirect 3.2 eV for anatase 3.0 eV for rutile
Carrier Mobility	100–300 $cm^2 V^{-1} s$	<1 $cm^2 V^{-1} s$
Crystalline Structure	Single crystalline	Mainly in polycrystalline
UV Adsorption	UVA absorption Broad spectrum adsorption	UVB absorption
Growth Mode	Anisotropic	Isotropic
Surface Mode	Mediate surface area	High surface area Ultra-high for anatase phase
Reference	(Mubeen et al., 2023) (Zhu & Wang, 2025)	(Etafa Tasisa et al., 2024) (Zhu & Wang, 2025)

Table 3. Kinetic rate of tofu and electroplating wastewater using resin immobilized photocatalyst TiO_2

Raw Water	Resin Immobilized Photocatalyst Mass (g)	Kinetic Model	Rate Constant (k)	Unit of k	R^2
Tofu Wastewater	10	First-Order	0.0059	1/min	0.9729
	20	First-Order	0.0076	1/min	0.9704
	30	First-Order	0.0093	1/min	0.9573
Electroplating	10	Second-Order	0.00000839	L/mg/min	0.9791
Wastewater	20	Second-Order	0.00000971	L/mg/min	0.9373
	30	Second-Order	0.00001278	L/mg/min	0.9255

thereby enabling visible light absorption and enhancing photocatalytic performance (Pesqueira et al., 2024) (Pan et al., 2015).

Kinetic Analysis of Photocatalytic Reactions in Tofu Wastewater and Electroplating Wastewater

Reaction kinetics analysis was conducted to understand the mechanism of pollutant removal rates during the photocatalytic process and to identify the most appropriate kinetic model for each type of wastewater. The kinetic approach provides important information regarding the relationship between pollutant concentration, reaction time, and the effect of using resin immobilized photocatalyst mass variation on the reaction rate. The results of the evaluation of the photocatalytic reaction kinetics in tofu wastewater and electroplating wastewater using using resin immobilized photocatalyst TiO_2 are presented in Table 3.

Based on Table 3, it can be seen that when using using resin immobilized photocatalyst TiO_2, tofu wastewater and electroplating wastewater undergo different processes in reaction kinetics. Tofu wastewater at different using resin immobilized photocatalyst mass variations has a first-order reaction, while electroplating wastewater tends to follow a second-order reaction. In general, photocatalysis kinetics are described using empirical models such as the pseudo-first-order and pseudo-second-order models derived from the general form of the Langmuir–Hinshelwood (L–H) equation. According to the L–H model, the degradation of a pollutant occurs through two main stages: adsorption of pollutant molecules on the catalyst surface and surface reactions involving reactive species, such as hydroxyl radicals (·OH) produced by electron-hole photoproduction (e^-–h^+) (Hikmah et al., 2025).

Under conditions where the pollutant concentration is relatively low and the active sites of the catalyst are not yet saturated, the reaction rate is usually proportional to the pollutant concentration, thus following first-order kinetics (pseudo-first-order). This is consistent with many literature reports on the degradation of dissolved organics, where the adsorption process

Table 4. Kinetic rate of tofu and electroplating wastewater treatment using resin immobilized photocatalyst ZnO

Raw Water	Resin Immobilized Photocatalyst Mass (g)	Kinetic Model	Rate Constant (k)	Unit of k	R^2
Tofu Wastewater	10	First-Order	0.0086	1/min	0.9910
	20	First-Order	0.0103	1/min	0.9804
	30	First-Order	0.0141	1/min	0.9938
Electroplating Wastewater	10	Second-Order	0.00000922	L/mg/min	0.9804
	20	Second-Order	0.00001188	L/mg/min	0.8858
	30	Second-Order	0.00001331	L/mg/min	0.8986

is not the main limiting factor and the reaction rate is mainly determined by the pollutant concentration itself. Conversely, pseudo-second-order kinetics may arise when the reaction rate depends on two factors simultaneously, such as the increasing contribution of strong adsorption, the involvement of reaction intermediates, or the interaction of two molecules on the catalyst surface. This is often seen in the degradation of inorganic pollutants or systems with more complex surface interactions, which cause the rate dependence to no longer be linear with respect to only one pollutant concentration (Tran et al., 2023).

These differences in kinetic behavior indicate that the rate-determining steps in the two wastewater systems studied are not identical. Tofu wastewater, which consists mainly of dissolved organic matter, tends to exhibit first-order kinetics, whereas electroplating wastewater containing Cr^{6+} ions exhibits behavior more consistent with second-order kinetics due to the strong adsorption of inorganic ions and the involvement of more complex surface reactions. This kinetic analysis provides deeper mechanistic insights into how using resin immobilized photocatalyst mass and pollutant properties affect the rate of photocatalytic reactions in each system.

In Table 4, the use of resin immobilized photocatalyst ZnO also shows the same behavior, namely the use of resin immobilized photocatalyst ZnO in the photocatalytic process in tofu wastewater makes it follow a first-order kinetic reaction and in electroplating wastewater it follows a second-order kinetic reaction. An interesting point to note is the reaction constant or k value. The k value for both resin immobilized photocatalyst TiO_2 and ZnO in tofu wastewater and electroplating wastewater tends to be directly proportional to the resin immobilized photocatalyst mass. It can be said that the greater the using resin immobilized photocatalyst mass, the higher the k value. This indicates that adding resin immobilized photocatalyst mass can increase the reaction rate.

Figure 5 shows the kinetic behavior of the photocatalytic reaction for each variation in resin immobilized photocatalyst mass given to tofu wastewater and electroplating wastewater. In tofu wastewater (Figures 5a and 5b), the linear relationship between $\ln(C_0/C)$ and time indicates that the elimination process follows first-order kinetics. An increase in using resin immobilized photocatalyst mass from 10 to 30 grams results in a steeper curve slope, indicating an increase in the reaction rate constant (k). However, changes in resin immobilized photocatalyst mass do not alter the reaction order but only affect the rate of the photocatalytic reaction. In electroplating wastewater (Figures 5c and 5d), the linear relationship between 1/Ca and time indicates that the Cr^{6+} reduction process is better modeled by second-order kinetics. Increasing the resin immobilized photocatalyst mass also increased the reaction rate, as indicated by the increased slope of the curve for both resin immobilized photocatalyst TiO_2 and ZnO. This behavior indicates that adding resin immobilized photocatalyst mass increases the number of active sites and the intensity of surface reactions that play a role in the Cr^{6+} reduction mechanism (Hassaan et al., 2023). In general, these results show that increasing the resin immobilized photocatalyst mass contributes to an increase in the reaction rate through an increase in surface area and the number of active sites, without changing the dominant kinetic mechanism of each type of wastewater.

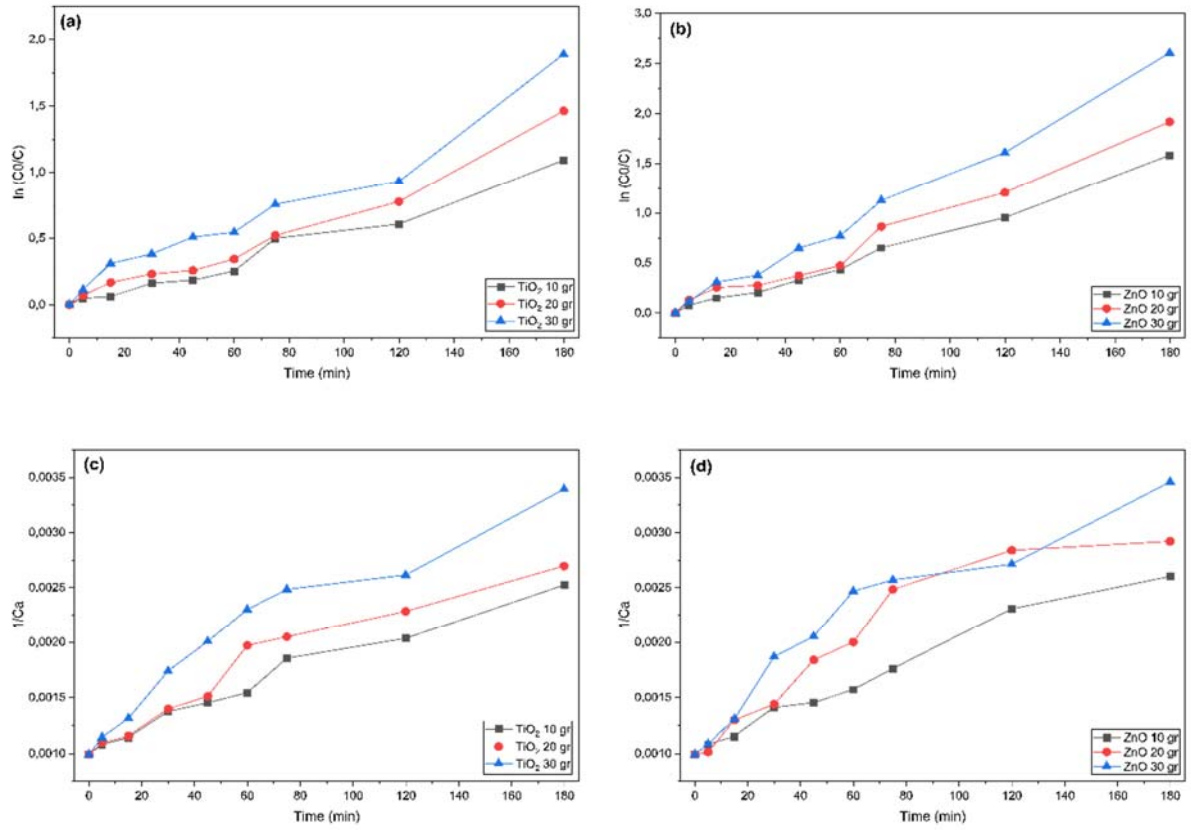

Fig. 5. Kinetic rate order using resin immobilized photocatalyst TiO_2 and ZnO in tofu and electroplating wastewater (a) TiO_2–tofu wastewater, (b) ZnO–tofu wastewater, (c) TiO_2–electroplating wastewater, and (d) ZnO–electroplating wastewater.

Operational Challenges and Optimization Strategies for Scale-Up Applications

A summary of previously published review articles is presented in Table 5 to provide an overview of the progress of this research compared to previous studies.

Current developments in photocatalysis technology no longer focus solely on improving reaction performance, but also begin to consider energy, material, and economic aspects simultaneously. This is evident from various studies showing that electricity consumption in UV-equipped photocatalysts remains the largest contributor to environmental impact and operational costs, and can even exceed 90% (Ngulube et al., 2025) (McKee & Chatzisymeon, 2022) (Notarnicola et al., 2023) (Pelayo et al., 2023). Efforts to reduce energy requirements, for example through the use of natural light sources such as solar-based photocatalysts, are indeed quite promising. However, this also raises another consequence increased environmental impact during the production stage of the catalyst material (Dubsok et al., 2022) (Sendão et al., 2025) (Maurya et al., 2023a) (Pookmanee et al., 2025).

In terms of materials, TiO_2 remains the primary choice due to its high stability and relatively low cost (Aghel et al., 2025) (Dihan et al., 2025). On the other hand, alternative materials such as g-C_3N_4 and various nanocomposites are increasingly being developed due to their ability to enhance photocatalytic performance (Sahoo et al., 2024) (Maurya et al., 2023b) (Safo et al., 2025). However, such performance improvements are generally accompanied by more complex synthesis processes and the potential for greater environmental impacts. Therefore, the integration of techno-economic assessment (TEA) and life-cycle assessment (LCA) is necessary to comprehensively evaluate the system, highlighting the dominance of precursor and ligand costs in advanced materials (G. Chen et al., 2025). Furthermore, these conditions

Table 5. Summary of recent studies on ZnO and TiO_2 based photocatalytic systems for wastewater treatment and their reported performance

Year	Title	Content	Reference
2025	A review on modified ZnO to address environmental challenges through photocatalysis: Photodegradation of organic pollutants	This review summarizes recent developments in ZnO-based nanomaterials for the photocatalytic degradation of organic contaminants. ZnO has a wide bandgap (3.37 eV) and exhibits rapid electron–hole recombination, which limits its performance. Therefore, various modification strategies such as doping, heterojunction formation, deposition, and radiation modification have been developed to enhance its efficiency.	(Rasheed et al., 2025)
2024	Photocatalytic activity enhancement of nanostructured metal-oxides photocatalyst: a review	The review summarizes nano-structured metal oxide semiconductors are promising photocatalysts due to their high photosensitivity, good chemical stability, non-toxicity, and biocompatibility. Recent developments indicate that ZnO-based nanocomposites are increasingly promising as photocatalytic materials for environmental remediation, energy conversion, and biomedical applications.	(Mohd Raub et al., 2024)
2021	ZnO Nanoadsorbents: A potent material for removal of heavy metal ions from wastewater	The review summarizes the use of ZnO nanostructures in removing toxic heavy metal ions from water was systematically reviewed. Various types of ZnO-based nanoadsorbents, including pure ZnO nanoparticles, doped ZnO, ZnO nanocomposites, and surface-modified ZnO, were thoroughly analyzed, including a comparison of maximum adsorption capacities for various heavy metal ions such as Cd^{2+}, Hg^{2+}, As^{3+}, Pb^{2+}, Cr^{6+}, Ni^{2+}, Co^{2+}, and Cu^{2+}.	(Dhiman & Kondal, 2021)
2026	Performance of resin immobilized photocatalyst-TiO_2 in treating wastewater containing hexavalent chromium	The review summarizes electroplating wastewater contains hazardous heavy metals, particularly Cr^{6+}. This study evaluated the effectiveness of TiO_2-immobilized resin (RIP-TiO_2) in a fixed-bed reactor with varying dosages (30–50 g) and contact times up to 180 minutes, using both real and synthetic wastewater under UV-C irradiation. The results showed removal efficiencies of 70.67% (real wastewater) and 37.64% (synthetic wastewater), with optimal performance at acidic pH and longer contact times.	(Hidayah et al., 2026)
2023	The Crosslinking and Porosity Surface Effects of Photoetching Process on Immobilized Polymer-Based Titanium Dioxide for the Decolorization of Anionic Dye	The review summarizes TiO_2 semiconductors immobilized in Epoxidized Natural Rubber (ENR) and Polyvinyl Chloride (PVC) were used via a dip-coating technique. Immobilization was carried out through a photoetching process for 0, 12, 24, and 30 hours. The photocatalytic process showed higher photocatalytic activity in the semiconductor samples that underwent the photolithography process, specifically in the 24-hour sample.	(Hamzah et al., 2023)
2022	Immobilization of resin photocatalyst in removal of soluble effluent organic matter and potential for disinfection by products	The review summarizes the performance of resin, as well as TiO_2 and ZnO-immobilized resin, in treating tofu wastewater. The results showed that all materials were capable of reducing dissolved organic matter (TOC and UV_{254}) by 93.45% and 76.51%, respectively, with the best performance demonstrated by RIP-ZnO, followed by RIP-TiO_2 and conventional resin. The reduction in SUVA indicates a change in the organic character of the wastewater consistent with the reduction in DBPs (THMs and HAAs). Thus, RIP-ZnO is the most promising option for wastewater treatment due to its high efficiency.	(Hidayah et al., 2022)

also drive more sustainable practices, such as the use of circular materials and the Material Properties and Sustainability (MAPS) framework to maintain a balance between performance and environmental impact (Aghel et al., 2025) (Costamagna et al., 2020) (Dihan et al., 2025) (Jia et al., 2025) (Shah & Gilbertson, 2024).

At the process level, no single reactor type can be considered the most superior for all conditions. Slurry systems provide better contact between the catalyst and the pollutant, but require an additional separation step. Conversely, immobilization systems are easier to operate continuously, but face challenges such as fouling, clogging, and mass diffusion limitations

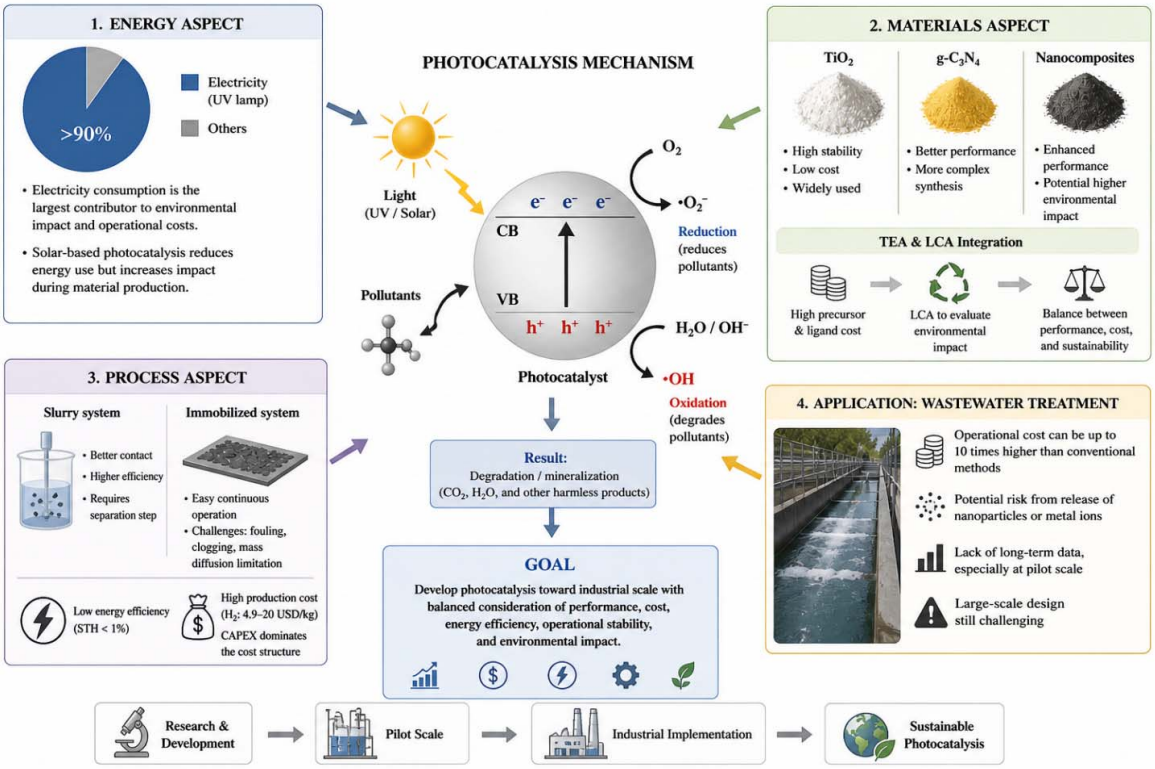

Fig. 6. Integrated Overview of Photocatalysis Mechanism with Techno-Economic, Environmental, and Process Challenges Toward Sustainable Industrial Scale

(Aghel et al., 2025) (Gowland et al., 2024). These challenges are exacerbated by the still-low energy efficiency (STH <1%) (Dihan et al., 2025) (Serik et al., 2026) which is far from the expected economic targets (Maurya et al., 2023b) (Qureshi & Tahir, 2024). The impact is evident in high production costs, including in energy applications such as hydrogen production, which remains in the range of 4.9–7.8 to approximately 20 USD/kg (Dihan et al., 2025) (Maurya et al., 2023b) as well as the dominance of CAPEX in the cost structure (Ngulube et al., 2024) (Alsayegh et al., 2019).

In wastewater treatment applications, the challenges faced are also significant. Operational costs can be up to ten times higher than those of conventional methods (Ngulube et al., 2025). Additionally, there is a potential environmental risk from the release of nanoparticles or metal ions during the process (Z. Chen et al., 2026) (Luo & Su, 2024) (Feijoo et al., 2020). The lack of long-term data, particularly at the pilot scale (Dominguez et al., 2018) (Pesqueira et al., 2020) also makes the design of large-scale systems still fraught with challenges. Overall, the development of photocatalysis toward an industrial scale still requires many adjustments. The focus is not only on improving reaction efficiency but also on energy efficiency, operational stability, and the selection of more environmentally friendly materials. A summary of the challenges and development directions is presented in Figure 6 and Table 6.

CONCLUSIONS

Based on the research results, a continuous photocatalytic system using immobilized TiO_2 and ZnO resins in a fixed-bed reactor was proven capable of effectively treating electroplating wastewater and tofu wastewater. The best performance was demonstrated by the immobilized

Table 6. Challenges and Development Pathways of Photocatalysis Toward Industrial Scale

Aspect	Key Finding	Major Challenges	Implications for Scale-up	Development Pathways / Solutions
Energy	Electricity consumption dominates environmental impacts (>90%), particularly in UV-based processes	Strong dependence on electrical energy and low light utilization efficiency (STH <1%)	High operational costs and increased carbon footprint, reducing industrial feasibility	Transition to renewable energy sources (e.g., solar), enhancement of photocatalyst efficiency, and optimization of irradiation systems
Materials	TiO_2 remains dominant, with emerging materials such as g-C_3N_4 and nanocomposites	Complex synthesis routes, high production costs, and potential greenhouse gas (GHG) emissions during manufacturing	Limitations in large-scale production and long-term material sustainability	Development of circular materials, utilization of waste/biomass-derived resources, and implementation of MAPS (Material Acceleration Platforms)
Economics	Production costs (e.g., H_2) range from 4.9–7.8 up to ~20 USD/kg, with CAPEX dominating total costs (75.6–89.7%)	Lack of competitiveness with conventional technologies and high initial investment requirements	Major barrier to commercialization and high financial risk in large-scale deployment	Process integration (e.g., with existing systems), design optimization, and techno-economic analysis (TEA)-driven strategies to reduce CAPEX and OPEX

ZnO resin, with a Cr^{6+} removal efficiency of 71.36% and a COD reduction of 92.61% at a mass of 30 g and an operating time of 180 minutes. Acidic pH conditions play a crucial role in enhancing hydroxyl radical (•OH) formation, thereby accelerating reduction and oxidation reactions. Additionally, differences in waste characteristics influence reaction mechanisms, with tofu waste following first-order kinetics, whereas electroplating waste follows second-order kinetics. This indicates that this photocatalyst is not only effective but also sufficiently adaptable to different types of pollutants.

Moving forward, this research can be further developed by varying the flow rate, as this affects residence time and the extent of optimal contact between pollutants and the catalyst within the reactor. Additionally, the use of alternative light sources, such as visible light or sunlight, is a viable option to reduce reliance on UV light while improving energy efficiency. This process can also be combined with subsequent stages, such as disinfection, to ensure that any remaining pathogenic microorganisms after the photocatalytic process are eliminated, making the effluent safer for discharge or reuse. On the other hand, economic analyses, such as a techno-economic assessment (TEA), are essential to determine whether this photocatalytic process is truly viable for industrial-scale application.

GRANT SUPPORT DETAILS

The authors acknowledge the financial support provided by the Institute for Research and Community Service, Universitas Pembangunan Nasional Veteran Jawa Timur, under the Undergraduate Thesis Funding Scheme (SPP/130/UN.63.8/LT/V/2025, May 7th, 2025).

CONFLICT OF INTEREST

The authors declare that there are no conflicts of interest influencing the publication of this manuscript. All ethical standards have been observed, including academic integrity, prevention of plagiarism, compliance with informed consent where applicable, avoidance of data fabrication and/or falsification, and prohibition of duplicate submission, publication, and redundancy.

LIFE SCIENCE REPORTING

This research poses no risks or threats related to life sciences. All research procedures were conducted in accordance with applicable ethical standards and did not involve materials, methods, or subjects that could endanger living organisms or the environment.

REFERENCES

Aghel, S., Bahramifar, N., Younesi, H., & Ziyarati, M. T. (2025). An integrated life cycle assessment of phenol photocatalytic degradation: Evaluating environmental and economic impacts of immobilized versus suspended TiO_2-based photocatalysts. J. Water Process Eng., 77; 108411.

Alsayegh, S., Johnson, J. R., Ohs, B., & Wessling, M. (2019). Methanol production via direct carbon dioxide hydrogenation using hydrogen from photocatalytic water splitting: Process development and techno-economic analysis. J. Clean. Prod., 208; 1446–1458.

Ananpattarachai, J., & Kajitvichyanukul, P. (2014). Kinetics and mass transfer of fixed bed photoreactor using N-doped TiO_2 thin film for tannery wastewater under visible light. Chem. Eng. Trans., 42; 163–168.

Azzahra, A. P., & Rahman, M. (2025). Removal efficiency of BOD, COD and TSS from tofu wastewater using an anaerobic system. Int. J. Res. Rev., 12(12); 54–62.

Castiblanco, Y., Perilla, A., Arbelaez, O., & Velásquez, P. (2021). Effect of the pH and the catalyst concentration on the removal of hexavalent chromium (Cr(VI)) during photocatalysis of wastewater from plating on plastics industry. Chem. Eng. Trans., 86; 679–684.

Chakravorty, A., & Roy, S. (2024). A review of photocatalysis, basic principles, processes, and materials. Sustain. Chem. Environ., 8; 100155.

Chen, G., Han, W., Lin, C., Li, Y., Zhou, S., & Kong, Y. (2025). Multifunctional Cu-engineered NH_2-MIL-125Ti@$ZnIn_2S_4$ heterojunction with dual-channel H_2O_2 activation for ultrafast water-mediated Cr(VI) photoreduction. Chem. Eng. J., 520; 165937.

Chen, Z., Zhao, C., Ma, R., Yao, Z., Guo, Z., Zhao, Z., Zheng, Y., & Fu, H. (2026). Interface and polarization engineering of ZIF-67(Co)-based heterojunctions for selective non-radical PMS activation. Adv. Funct. Mater., 36(12); e16474.

Cloteaux, A., Gérardin, F., Thomas, D., Midoux, N., & André, J.-C. (2014). Fixed bed photocatalytic reactor for formaldehyde degradation: Experimental and modeling study. Chem. Eng. J., 249; 121–129.

Costamagna, M., Ciacci, L., Paganini, M. C., Calza, P., & Passarini, F. (2020). Combining the highest degradation efficiency with the lowest environmental impact in zinc oxide based photocatalytic systems. J. Clean. Prod., 252; 119762.

Dhiman, V., & Kondal, N. (2021). ZnO nanoadsorbents: A potent material for removal of heavy metal ions from wastewater. Colloid Interface Sci. Commun., 41; 100380.

Dihan, M. R., Rahman, T. U., Jaman Riad Khan, M. A., Banhi, T. S., Sadaf, S., Reza, M. S., Afroze, S., Islam, S. Z., & Islam, M. S. (2025). Photocatalytic and photoelectrochemical H_2 generation for sustainable future. Fuel, 392; 134356.

Dimitropoulos, M., Aggelopoulos, C. A., Sygellou, L., Tsantis, S. T., Koutsoukos, P. G., & Yannopoulos, S. N. (2024). Unveiling the photocorrosion mechanism of zinc oxide photocatalyst. J. Environ. Chem. Eng., 12(2); 112102.

Dominguez, S., Laso, J., Margallo, M., Aldaco, R., Rivero, M. J., Irabien, Á., & Ortiz, I. (2018). LCA of greywater management within a circular economy framework. Sci. Total Environ., 621; 1047–1056.

Dubsok, A., Khamdahsag, P., & Kittipongvises, S. (2022). Life cycle environmental impact assessment of cyanate removal in mine tailings wastewater. J. Clean. Prod., 366; 132928.

Dworschak, D., Brunnhofer, C., & Valtiner, M. (2020). Photocorrosion of ZnO single crystals during electrochemical water splitting. ACS Appl. Mater. Interfaces, 12(46); 51530–51536.

Elystia, S., HS, E., & Karamy, A. G. (2021). Penyisihan logam Cr(VI) dari limbah cair elektroplating menggunakan mikroalga *Chlorella* sp. dengan variasi penambahan external-glutathione. J. Serambi Eng., 6(1); 1522–1528.

Etafa Tasisa, Y., Kumar Sarma, T., Krishnaraj, R., & Sarma, S. (2024). Band gap engineering of titanium dioxide (TiO_2) nanoparticles prepared via green route for environmental remediation. Results Chem., 11; 101850.

Fatehah, M. O., Aziz, H. A., & Stoll, S. (2014). Stability of ZnO nanoparticles in solution: Influence of pH, dissolution, aggregation and disaggregation effects. J. Colloid Sci. Biotechnol., 3(1); 75–84.

Feijoo, S., González-Rodríguez, J., Fernández, L., Vázquez-Vázquez, C., Feijoo, G., & Moreira, M. T. (2020). Fenton and photo-Fenton nanocatalysts revisited from the perspective of life cycle assessment. Catalysts, 10(1); 23.

Ge, J., Zhang, Z., Ouyang, Z., Shang, M., Liu, P., Li, H., & Guo, X. (2022). Photocatalytic degradation of (micro)plastics using TiO_2-based and other catalysts. Environ. Res., 209; 112729.

Gowland, D. C. A., Robertson, N., & Chatzisymeon, E. (2024). Life cycle assessment of immobilised and slurry photocatalytic systems for removal of natural organic matter. Environments, 11(6); 114.

Hamzah, S. R., Rosli, M. A., Natar, N. S., Ghani, N. I. A., Muhamad, N. A., Azami, M. S., Ishak, M. A. M., Nordin, R., & Nawawi, W. I. (2023). Crosslinking and porosity surface effects of photoetching process on immobilized polymer-based TiO_2. Colorants, 2(1); 73–89.

Hardyanti, N., Susanto, H., & Budihardjo, M. A. (2024). Removal of organic matter from tofu wastewater using adsorption, Fenton oxidation, and ultrafiltration. Desalin. Water Treat., 318; 100255.

Hardyanti, N., Susanto, H., Budihardjo, M. A., & Saputra, A. T. (2023). Characteristics of tofu wastewater from different soybeans and production stages. Ecol. Eng. Environ. Technol., 24(8); 54–63.

Hassaan, M. A., El, M. A., & Marwa, N. (2023). Principles of photocatalysts and their applications: A review. Top. Curr. Chem., 381(6); 44.

Hidayah, E. N., Laili, N., Mukharomah, A., Cahyonugroho, O. H., & Puspitawati, I. N. (2026). Performance of resin immobilized photocatalyst-TiO_2 in treating wastewater containing hexavalent chromium. J. Ecol. Eng., 27(2); 357–370.

Hidayah, E. N., Pachwarya, R. B., & Cahyonugroho, O. H. (2022). Immobilization of resin photocatalyst in removal of soluble effluent organic matter. Glob. J. Environ. Sci. Manag., 8(3); 437–448.

Hikmah, R., Murti, A., Abdus, M., Jawwad, S., Ayuningtiyas, K. K., & Hidayah, E. N. (2025). High efficiency on resin photocatalysis: Application and kinetic mechanism using Langmuir–Hinshelwood model. S. Afr. J. Chem. Eng., 53; 87–95.

Illahi, A. N., Rouf, U. A., Maulidianingtyas, H., Hastuti, E., Prasetyo, A., & Istighfarini, V. N. (2020). Sintesis dan karakterisasi material fotokatalis heterojunction $Bi_4Ti_3O_{12}/SrTiO_3$. J. Kim. Ris., 5(1); 36–43.

Iyyappan, J., Gaddala, B., Gnanasekaran, R., Gopinath, M., Yuvaraj, D., & Kumar, V. (2024). Critical review on wastewater treatment using photocatalytic AOP. Case Stud. Chem. Environ. Eng., 9; 100599.

Jasim, A. Q., & Ajjam, S. K. (2024). Removal of heavy metal ions using ion exchange resin in batch process. S. Afr. J. Chem. Eng., 49; 43–54.

Jia, H., Yang, Y., Zhang, Y., Li, Z., Yu, H., Zhang, Y., Lu, Y., & Zhou, D. (2025). Synergy of adsorption and photocatalysis in UiO-66/g-C_3N_4 system. Sep. Purif. Technol., 369; 133119.

Jiang, B., Gong, Y., Gao, J., Sun, T., Liu, Y., Oturan, N., & Oturan, M. A. (2019). Reduction of Cr(VI) to Cr(III) mediated by carboxylic acids. J. Hazard. Mater., 365; 266–303.

Kotze, M., Green, B., Mackenzie, J., & Virnig, M. (2016). Resin-in-pulp and resin-in-solution. Gold Ore Process., 561–583.

Lee, H., Park, J., Lam, S. S., Park, Y.-K., Kim, S.-C., & Jung, S.-C. (2022). Diclofenac degradation using La-doped TiO_2 photocatalyst. Sustain. Chem. Pharm., 25; 100564.

León-Condés, C. A., Martínez-Barrera, G., & Roa-Morales, G. (2022). Green nanocomposites and gamma radiation as a novel treatment for dye removal in wastewater. Elsevier, Chap. 12; 323–339.

Li, X., Wei, H., Song, T., Lu, H., & Wang, X. (2023). Photocatalytic degradation of organic pollutants in water by modified TiO_2: A review. Water Sci. Technol., 88(6); 1495–1507.

Li, Z., & Du, C. (2025). Current status and research trends of electroplating wastewater treatment. Desalination, 613; 119004.

Luo, Y., & Su, R. (2024). Environmental impact of waste treatment and hydrogen production based on LCA. Toxics, 12(9); 652.

Ma, X., Li, H., Liu, T., Du, S., Qiang, Q., Wang, Y., Yin, S., & Sato, T. (2017). Comparison of photocorrosion and selective corrosion in Ag-ZnO. Appl. Catal. B Environ., 201; 348–358.

Maurya, J., Gemechu, E., & Kumar, A. (2023a). Life cycle assessment of earth-abundant photocatalysts for hydrogen production. Int. J. Hydrog. Energy, 48(52); 20077–20095.

Maurya, J., Gemechu, E., & Kumar, A. (2023b). Techno-economic assessment models for hydrogen production via photocatalysis. Energy Convers. Manag., 279; 116750.

McKee, S. M., & Chatzisymeon, E. (2022). Environmental sustainability of LED and blacklight lamps for water treatment. Environ. Impact Assess. Rev., 97; 106886.

Miri-Jahromi, A., Mohammady Maklavany, D., Rouzitalab, Z., Ghaemi Khiavi, S., Ghasemy, E., Khedri, M., Rezvantalab, S., Sharafinia, S., Rashidi, A., & Maleki, R. (2022). Engineering of two-dimensional monolayers for phenolic compound removal. J. Mol. Liq., 362; 119784.

Mohd Raub, A. A., Bahru, R., Mohamed, M., Latif, R., Haniff, M., Simarani, K., & Yunas, J. (2024). Photocatalytic activity enhancement of nanostructured metal-oxides. Nanotechnology, 35; ad33e8.

Mubeen, K., Irshad, A., Safeen, A., Aziz, U., Safeen, K., Ghani, T., Khan, K., Ali, Z., Haq, I. ul, & Shah, A. (2023). Band structure tuning of ZnO/CuO composites. J. Saudi Chem. Soc., 27; 101639.

Navidpour, A. H., Abbasi, S., Li, D., Mojiri, A., & Zhou, J. L. (2023). Advanced oxidation process using TiO_2 semiconductor photocatalyst. Catalysts, 13; 232.

Ngulube, K. F., Abdelhaleem, A., Fujii, M., & Nasr, M. (2024). ZnO@$Mg(OH)_2$ nanocomposite for photocatalytic degradation. J. Water Process Eng., 64; 105605.

Ngulube, K. F., Abdelhaleem, A., Osman, A. I., Peng, L., & Nasr, M. (2025). Sustainable water treatment using magnetite-based photocatalysts. Environ. Sci. Pollut. Res., 32(49); 28159–28195.

Notarnicola, B., Tassielli, G., Renzulli, P. A., Di Capua, R., Astuto, F., Mascolo, G., Murgolo, S., De Ceglie, C., Curri, M. L., Comparelli, R., & Dell'Edera, M. (2023). LCA of UV-C wastewater treatment systems. Sci. Total Environ., 857; 159309.

Pan, J. W., Li, C., Zhao, Y. F., Liu, R. X., Gong, Y. Y., Niu, L. Y., Liu, X. J., & Chi, B. Q. (2015). Electronic properties of doped TiO_2. Chem. Phys. Lett., 628; 43–48.

Pelayo, D., Rivero, M. J., Santos, G., Gómez, P., & Ortiz, I. (2023). Techno-economic evaluation of UV light technologies. Sci. Total Environ., 868; 161376.

Pesqueira, J. F. J. R., Pereira, M. F. R., & Silva, A. M. T. (2020). Environmental impact of advanced wastewater treatment technologies. J. Clean. Prod., 261; 121078.

Pesqueira, J. F. J. R., Pereira, M. F. R., & Silva, A. M. T. (2024). Carbon-based composites in wastewater treatment. J. Clean. Prod., 444; 140845.

Pookmanee, P., Promwanna, K., Sangsrichan, S., Kitikul, J., Thanomwat, M., Chaiwoot, P., Kruefu, V., Ubolsook, P., & Jansanthea, P. (2025). Nitrogen-doped TiO_2 synthesis and LCA. ChemistrySelect, 10(35); e03820.

Prasad, S., Kumar, K., Kumar, S., Gupta, N., Marina, M., Cabral-Pinto, S., Rezania, S., Radwan, N., & Alam, J. (2021). Chromium contamination and environmental health effects. J. Environ. Manag., 285; 112174.

Prawati, P., Oktariany, A., Putri, S. S., Aditya, I., & Kartohardjono, S. (2019). Tofu wastewater treatment using coagulation and ultrafiltration. IOP Conf. Ser. Mater. Sci. Eng., 703; 012013.

Qu, W., Louangsouphom, B., Ye, X., Liu, H., & Wang, X. (2025). Macroporous resin-based TiO_2 composites for pollutant removal. Catalysts, 15(8); 759.

Qureshi, F., & Tahir, M. (2024). Photoelectrochemical water splitting for hydrogen production. Int. J. Hydrog. Energy, 69; 760–776.

Ramadhika, L. N., Aprilia, A., & Safriani, L. (2021). Studi preparasi senyawa ZnO:TiO_2 sebagai material fotokatalis. J. Mater. Energi Indones., 11(2); 83–95.

Rangarajan, G., Jayaseelan, A., & Farnood, R. (2022). Photocatalytic reactive oxygen species generation for pollutant removal. J. Clean. Prod., 346; 131155.

Rasheed, H. M., Aroosh, K., Meng, D., Ruan, X., Akhter, M., & Cui, X. (2025). Modified ZnO for environmental photocatalysis applications. Mater. Today Energy, 48; 101774.

Ren, G., Han, H., Wang, Y., Liu, S., Zhao, J., Meng, X., & Li, Z. (2021). Recent advances of photocatalytic applications in water treatment. Nanomaterials, 11(7); 1804.

Safo, K., Rubangakene, N. O., Noby, H., & El-Shazly, A. H. (2025). Photocatalytic purification using hybrid TiO_2 nanocomposite. Water Sci. Eng., 18(2); 151–164.

Sahoo, S., Mahamallik, P., Das, R., & Panigrahi, S. (2024). Non-metal doped g-C_3N_4 photocatalyst for pollutant remediation. Environ. Res., 258; 119390.

Sendão, R. M. S., Esteves da Silva, J. C. G., & Pinto da Silva, L. (2025). Life cycle assessment of TiO_2-carbon dots nanocomposites. NanoImpact, 38; 100556.

Serik, A., Kuspanov, Z., & Daulbayev, C. (2026). Cost-effective strategies for green hydrogen production. Renew. Sustain. Energy Rev., 226; 116242.

Shah, Y., & Gilbertson, L. M. (2024). Environmental impact of graphitic carbon nitride materials. Environ. Sci. Nano, 11(1); 78–90.

Shan, A., Lu, Y., Cheng, L., Hou, Z., Xili, D., Li, Y., Liu, J., Ma, H., & Yang, J. (2023). Enhanced degradation of photogenerated holes in TiO_2 systems. Mater. Today Sustain., 22; 100391.

Silmina, S., Wu, X., Rolle, C., Chen, F., Wang, H., & Khairunnisa, S. (2023). Photocatalytic reduction of Cr(VI) using graphene quantum dots. Sci. Eng. Technol., 3(2); 1–11.

Szabó, M., Kalmár, J., Ditrói, T., Bellér, G., Lente, G., Simic, N., & Fábián, I. (2018). Chromium(VI) speciation in aqueous solution. Inorg. Chim. Acta, 472; 295–301.

Taylor, C. M., Ramirez-Canon, A., Wenk, J., & Mattia, D. (2019). Enhancing photocorrosion resistance of ZnO nanowires. J. Hazard. Mater., 378; 120799.

Tran, H. D., Nguyen, D. Q., Do, P. T., & Tran, U. N. P. (2023). Kinetics of photocatalytic degradation of organic compounds. RSC Adv., 13(25); 16915–16925.

Ul, Z., Khan, H., Shad, N., Sabahat, S., Sun, J., Tahir, K., Samad, N., Muhammad, N., Rahim, A., Imran, M., Iqbal, J., Malook, T., Khasim, S., Farooq, U., & Wu, J. (2023). Removal of organic pollutants through hydroxyl radical-based AOPs. Ecotoxicol. Environ. Saf., 267; 115564.

Wise, J. P., Young, J. L., Cai, J., & Cai, L. (2022a). Current understanding of hexavalent chromium neurotoxicity. Environ. Int., 158; 106877.

Wise, J. P., Young, J. L., Cai, J., & Cai, L. (2022b). Current understanding of hexavalent chromium neurotoxicity. Environ. Int., 158; 106877.

Yang, H., & Chen, J. (2024). Photocatalytic fixed bed reactions for contaminant mineralization. J. Environ. Chem. Eng., 12(3); 112765.

Yu, L., Chen, W., Li, D., Wang, J., Shao, Y., He, M., Wang, P., & Zheng, X. (2015). Inhibition of photocorrosion in ZnO via ZnO/ZnS structure. Appl. Catal. B Environ., 164; 453–461.

Zahrah, A. A., Purnomo, Y. S., & Ayu, R. H. M. (2025). Efisiensi pengolahan Cr(VI) dengan resin immobilized photocatalyst technology. Serambi Eng., 10(1); 11819–11825.

Zakria, H. S., Othman, M. H. D., Kamaludin, R., Sheikh Abdul Kadir, S. H., Kurniawan, T. A., & Jilani, A. (2021). Immobilization techniques of photocatalyst on polymer membrane. RSC Adv., 11(12); 6985–7014.

Zeng, R., Mannaerts, C. M., & Lievens, C. (2023). UV-VIS spectra analysis for CDOM absorption properties. Front. Environ. Sci., 11; 1152536.

Zheng, X. (2022). Application of nano-TiO_2 photocatalyst in marine pollution control. Desalin. Water Treat., 268; 303–312.

Zhu, C., & Wang, X. (2025). ZnO nanomaterials synthesis and photocatalytic applications. Nanomaterials, 15; 628.